

# Global Biogeochemical Cycles

## RESEARCH ARTICLE

10.1029/2018GB006110

### Key Points:

- We estimate a contribution of pteropods to shallow (100 m) export of  $\text{CaCO}_3$  of at least 33% and to pelagic calcification of up to 89%
- The simulation that agrees with all the observations has a  $\text{CaCO}_3$  production of 4.7 Pg C/year but  $\text{CaCO}_3$  export at 100 m of only 0.6 Pg C/year

### Correspondence to:

E. T. Buitenhuis,  
e031@uea.ac.uk

### Citation:

Buitenhuis, E. T., Le Quéré, C., Bednaršek, N., & Schiebel, R. (2019). Large contribution of pteropods to shallow  $\text{CaCO}_3$  export. *Global Biogeochemical Cycles*, 33, 458–468. <https://doi.org/10.1029/2018GB006110>

Received 16 OCT 2018

Accepted 21 FEB 2019

Accepted article online 23 FEB 2019

Published online 20 MAR 2019

## Large Contribution of Pteropods to Shallow $\text{CaCO}_3$ Export

Erik T. Buitenhuis<sup>1</sup> , Corinne Le Quéré<sup>1</sup> , Nina Bednaršek<sup>2</sup> , and Ralf Schiebel<sup>3</sup> 

<sup>1</sup>Tyndall Centre for Climate Change Research, School of Environmental Sciences, University of East Anglia, Norwich, UK, <sup>2</sup>Southern California Coastal Water Research Authority, Costa Mesa, CA, USA, <sup>3</sup>Department of Climate Geochemistry, Max Planck Institute for Chemistry, Mainz, Germany

**Abstract** The literature on the relative contributions of pelagic calcifying taxa to the global ocean export of  $\text{CaCO}_3$  is divided. Studies based on deep sediment trap data tend to argue that either foraminifers or coccolithophores, both calcite producers, dominate export. However, the compilations of biomass observations for pteropods, coccolithophores, and foraminifers instead show that pteropods dominate the global ocean calcifier biomass and therefore likely also carbonate export. Here we present a new global ocean biogeochemical model that explicitly represents these three groups of pelagic calcifiers. We synthesize databases of the physiology of the three groups to parameterize the model and then tune the unconstrained parameters to reproduce the observations of calcifier biomass and  $\text{CaCO}_3$  export. The model can reproduce both these observational databases; however, substantial dissolution of aragonite above the aragonite saturation horizon is required to do so. We estimate a contribution of pteropods to shallow (100 m) export of  $\text{CaCO}_3$  of at least 33% and to pelagic calcification of up to 89%. The high production-high dissolution configuration that shows closest agreement with all the observations has a  $\text{CaCO}_3$  production of 4.7 Pg C/year but  $\text{CaCO}_3$  export at 100 m of only 0.6 Pg C/year.

**Plain Language Summary** We show that pteropods contribute at least 33% to export of  $\text{CaCO}_3$  at 100m and up to 89% to pelagic calcification. This is in line with results by Betzer et al., 1984 and Byrne et al., 1984, and contradicts most of the work that has been published since then, which has tended to argue for the dominance of either coccolithophores or foraminifers. Pteropods precipitate  $\text{CaCO}_3$  in the crystal form of aragonite. This is more soluble than calcite, which is produced by coccolithophores and pelagic foraminifers. Thus, the ocean alkalinity cycle and associated buffer capacity for  $\text{CO}_2$  could be more sensitive to rising  $\text{CO}_2$  than has been suggested by existing Earth System Models, which only represent calcite.

## 1. Introduction

It has long been noted that there is an inconsistency between estimates of pelagic  $\text{CaCO}_3$  production and the smaller flux of  $\text{CaCO}_3$  that is found in bottom-tethered sediment traps (Berelson et al., 2007; Milliman et al., 1999). Several potential explanations have been put forward to explain this inconsistency, which include shallow dissolution in acidic microenvironments (Buitenhuis et al., 1996; Milliman et al., 1999; Schiebel et al., 2007), and the production of soluble aragonite by pteropods that is dissolved before it reaches deep sediment traps (Betzer et al., 1984; Byrne et al., 1984). Milliman et al. (1999) rejected this latter potential explanation in their review of the marine carbonate budget, based on the low contribution of pteropods to total  $\text{CaCO}_3$  production measured by Fabry (1990). However, the latter paper contains only three data points in the low-latitude Northeast Pacific Ocean, and more data have since become available.

Here we reexamine the relative contribution of the different groups of calcifying organisms in the total carbonate budget, by contrasting bottom-up data from turnover rates and biomass measurements (described below) with top-down data from sediment traps (Torres Valdés et al., 2014). The recent publication of the MARine Ecosystem DATa (MAREDAT) atlas of plankton biomass distributions of 10 plankton functional types (PFTs) has provided one part of the necessary global information. It includes compilations of biomass observations for pteropods (Bednaršek et al., 2012), coccolithophores (O'Brien et al., 2013), and foraminifers (Schiebel & Movellan, 2012). Comparison of these databases show that pteropods dominate the global ocean calcifier biomass (Buitenhuis, Vogt, et al., 2013) and therefore possibly also carbonate export. Here we add a synthesis of the turnover rates of the three calcifying PFTs that are represented in MAREDAT: pteropods,

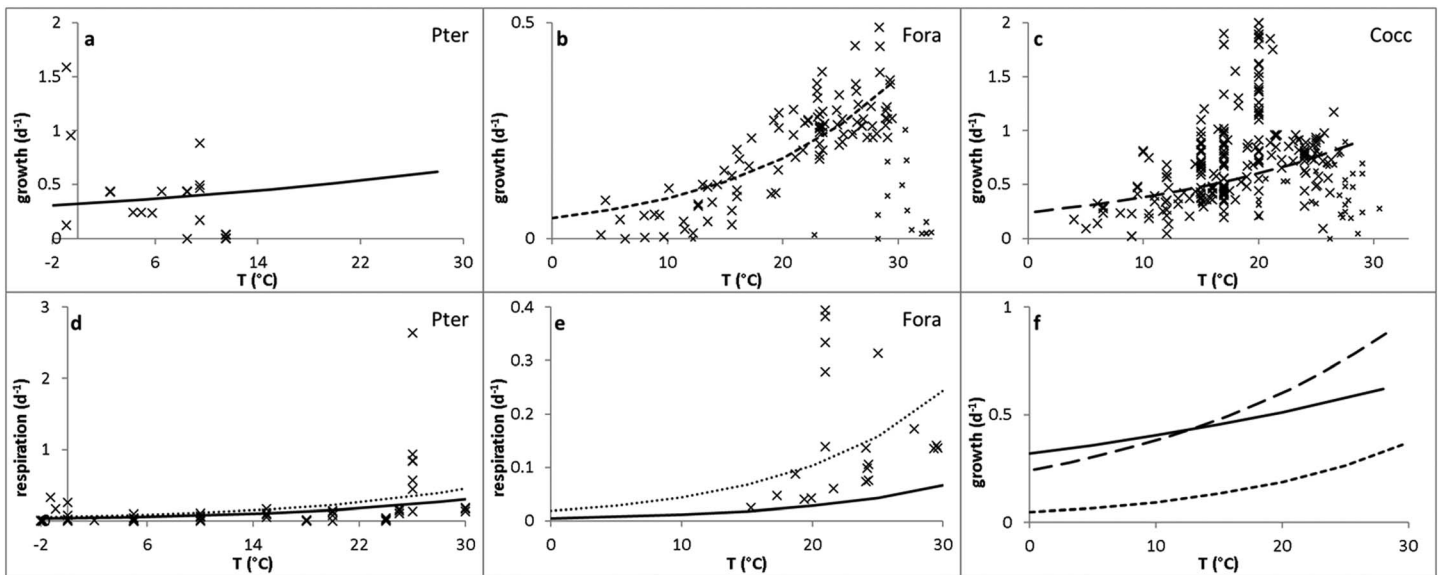


**Figure 1.** Turnover rates of calcifying plankton functional types. (a) Pteropod growth rate. (b) Foraminifer growth rate. (c) Coccolithophore growth rate. (d) Pteropod respiration. (d, e) Dotted line: fit to the data. Solid line: function used in the model. (e) Foraminifer respiration rate. (f) Plankton functional type comparison of fitted growth rates. Solid line: pteropods. Short dash: foraminifers. Long dash: coccolithophores. Growth rates above the optimum temperature for each species (small symbols) have been excluded from the fits.

coccolithophores, and foraminifers. With this information, we extend a global biogeochemical model to represent these PFTs and use the model to test whether the production and shallow dissolution of pteropod aragonite might reasonably reconcile the relatively large surface ocean  $\text{CaCO}_3$  production rate of 1.1–1.6 Pg C/year (Berelson et al., 2007; Lee, 2001) with the lower export at 2,000-m depth of  $0.6 \pm 0.4$  Pg C/year (Berelson et al., 2007) or 0.4 Pg C/year (Honjo et al., 2008), well above the calcite saturation horizon.

We also examine whether our results support or contradict  $\text{CaCO}_3$  dissolution above the aragonite saturation horizon. Feely et al. (2004) argued for substantial  $\text{CaCO}_3$  dissolution above the saturation horizon based on the  $\text{TA}^*$  method, which estimates the part of excess alkalinity that is caused by  $\text{CaCO}_3$  dissolution and divides it by water age estimated from CFC or  $^{14}\text{C}$  concentrations. However, Friis et al. (2006) showed this method to be inconclusive, because it does not account for physical transport of excess  $\text{TA}^*$  into supersaturated waters.

## 2. Model Description

For this study, we produced the global ocean biogeochemical model PlankTOM12. It was based on the PlankTOM10 model described by Le Quéré et al. (2016), which explicitly represents six types of phytoplankton, including coccolithophores, three size classes of zooplankton, and picoheterotrophs (*Bacteria + Archaea*). We have extended PlankTOM to include representations of two further zooplankton PFTs (zPFTs): calcifying pteropods and foraminifers. These zPFTs have the same basic behavioral and biogeochemical structure as the other zooplankton in the model, but in addition, they calcify: pteropods producing aragonite and foraminifers producing calcite. PlankTOM12 represents full cycles of C, N, P, Si, Alkalinity,  $\text{O}_2$ , and chlorophyll, and a simplified cycle of Fe. Considerable effort has gone into basing the PlankTOM model series on physiological and ecological observations and validating it against environmental observations (Buitenhuis, Hashioka, et al., 2013; Buitenhuis et al., 2010, 2006; Le Quéré et al., 2005, 2016). For a full description, including equations, see Enright and Buitenhuis (2014).

The grazing rates of zPFTs are dependent on food availability, temperature, and predator biomass. The resultant grazing flux is partitioned across growth, respiration, and particulate organic carbon (POC) and dissolved organic carbon (DOC) egestion, with respiration split between basal respiration and food respiration that is proportional to grazing (Buitenhuis et al., 2010; Le Quéré et al., 2016).  $\text{CaCO}_3$

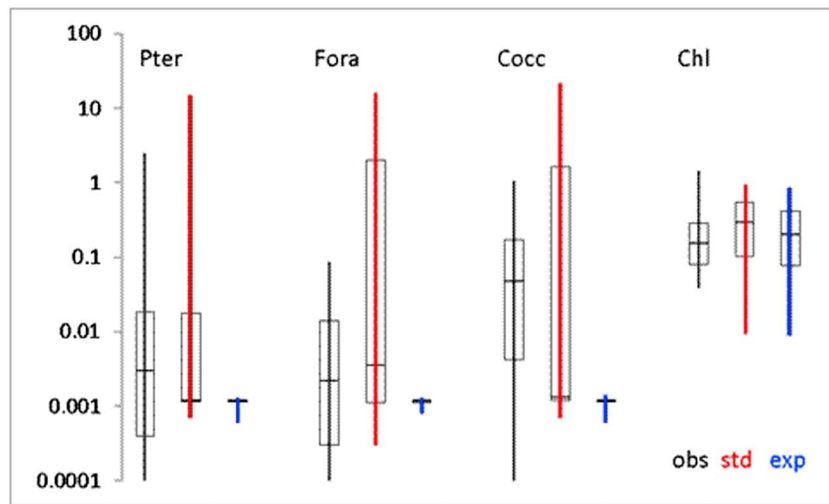


**Figure 2.** Frequency distribution of calcifier biomass ( $\mu\text{g C/L}$ ) and chlorophyll ( $\mu\text{g/L}$ ). Lines connect 5th and 95th percentiles. Bottom of boxes: 25th percentile. Middle line in boxes: median. Top of boxes: 75th percentiles. Fifth percentiles of the biomass observations are 0. PTE = pteropods; FOR = foraminifers; COC = coccolithophores; CHL = chlorophyll; obs = observations; std = standard model run; exp = optimized to reproduce  $\text{CaCO}_3$  export without dissolution above the saturation horizons. Model results have been sampled where there are observations.

production is proportional to organic carbon production and growth. Detrital  $\text{CaCO}_3$  from zooplankton is generated in the same way as from coccolithophores: A fixed proportion is lost during respiration and grazing by other zooplankton—even if this is above the saturation horizon—and the rest acts as ballast in the fast-sinking particles (Buitenhuis, Hashioka, et al., 2013). The density of aragonite (produced by pteropods) was taken to be the same as the density of calcite (produced by coccolithophores and foraminifers, Buitenhuis et al., 2001). Chemical dissolution rates proportional to the level of undersaturation were modeled as previously described for aragonite (Gangstø et al., 2008) and calcite (Gehlen et al., 2007).

The biogeochemical model was incorporated into the Ocean General Circulation Model NEMO (Madec, 2008). NEMO was updated to version 3.5. The model was initialized with observations (Le Quéré et al., 2016) and run from 1990 to 2014, forced with atmospheric conditions from ECMWF (European Centre for Medium-range Weather Forecasts) reanalysis. We present the average of the last 5 years of simulation.

### 3. Data Description for Model Parameterization

#### 3.1. Turnover Rates

We compiled physiological data on respiration and on food-saturated growth or grazing rates as a function of temperature for pteropods and foraminifers (Figure 1) from the literature (Bednaršek et al., 2016; Le Quéré et al., 2016; Lombard et al., 2009, 2011). There are few measurements of pteropod growth rates, and only below  $12^\circ\text{C}$  (Figure 1a), so that a fit to the data was unrealistic ( $Q_{10} = 0.3$ ). The growth rates are similar to the relationship that was derived for mesozooplankton, so we used the same relationship in the model (Figure 1a). Pteropods are of similar size or slightly smaller than copepods, which are the basis for the growth relationship for mesozooplankton, so copepod growth rates would be expected to be representative for pteropods. We compiled data on the  $\text{CaCO}_3$ :POC ratio in pteropods as  $0.52 \pm 0.24$  mol/mol ( $n = 5$  only). The  $\text{CaCO}_3$ :POC ratio in coccolithophores was taken as  $0.10 \pm 0.05$  mol/mol ( $n = 127$ , Heinle, 2013), and in foraminifers as  $0.49 \pm 0.50$  mol/mol ( $n = 549$ , Schiebel & Movellan, 2012). We could not find data on gross growth efficiency and the fraction of grazing that is egested as DOC and POC for pteropods or foraminifers. Gross growth efficiency is indistinguishable between zooplankton groups (Moriarty, 2009). Therefore, we used the averages for all mesozooplankton (GGE = 0.26, fraction POC = 0.30, fraction DOC when basal respiration is negligible = 0.14) for pteropods and for all protozoan zooplankton (GGE = 0.30, fraction POC = 0.13, fraction DOC when basal respiration is negligible = 0.28) for foraminifers.

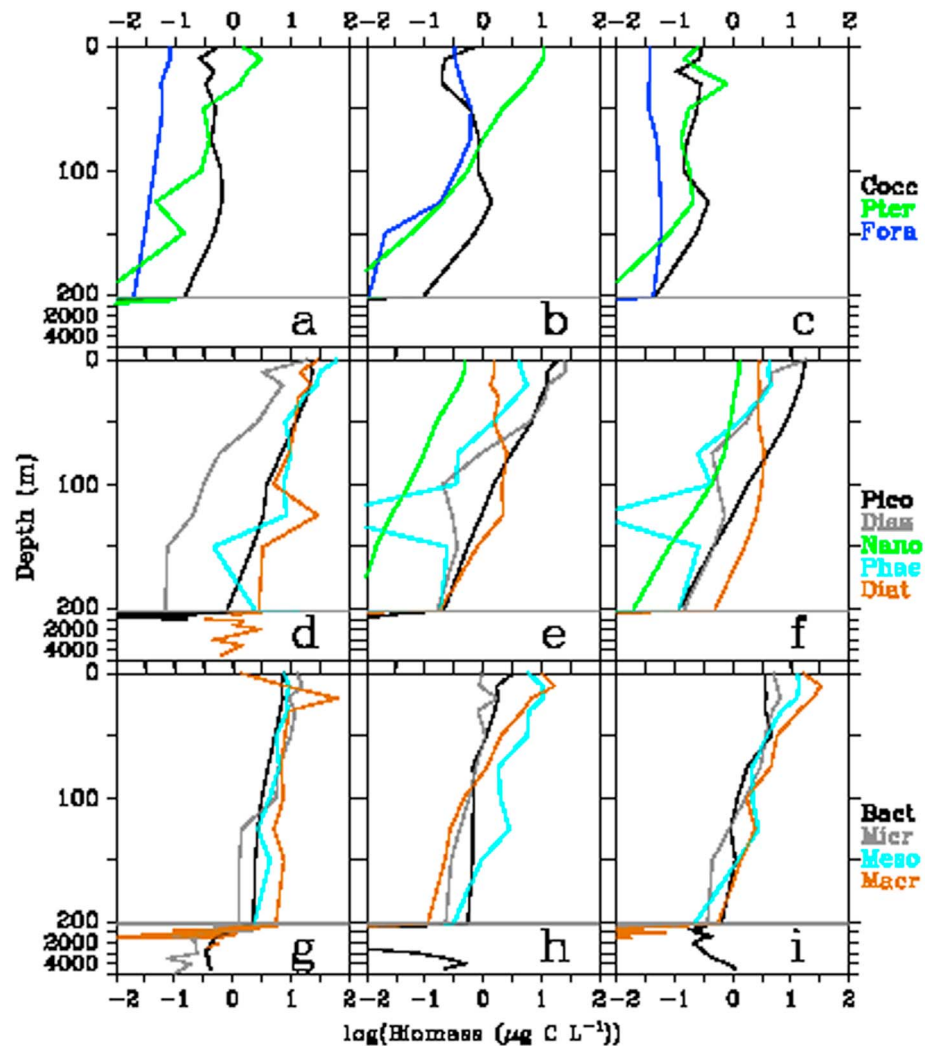


**Figure 3.** Vertical profiles of log (plankton functional type biomass,  $\mu\text{g C/L}$ ). Model results have been sampled where there are observations. Gray horizontal lines separate the upper ocean with generally good data coverage from the deep ocean with generally poorer data coverage. (a–c) Calcifiers: Cocc = coccolithophores; Pter = pteropods; Fora = foraminifers. (d–f) Other autotrophs: Pico = picophytoplankton; Diaz =  $\text{N}_2$  fixers; Nano = nanophytoplankton; Phae = *Phaeocystis sp.*; Diat = diatoms. (g–i) Other heterotrophs: Bact = *Bacteria* + *Archaea*; Micr = microzooplankton; Meso = mesozooplankton; Macr = macrozooplankton. (a, d, g) MAREDAT2012 observations (Buitenhuis, Vogt, et al., 2013). (b, e, h) Standard model run. (c, f, i) Model tuned to reproduce  $\text{CaCO}_3$  export without dissolution above the saturation horizons.

To evaluate the model, we compiled a small database from the literature ( $n = 43$ , Berner & Honjo, 1981, Betzer et al., 1984, Fabry, 1989, 1990, Fabry & Deuser, 1991) of in situ pteropod production, aragonite flux in sediment traps, and the fraction that this aragonite flux makes up of the total  $\text{CaCO}_3$  flux.

### 3.2. Food Preferences and Biomass Distributions

For zooplankton, ecosystem interactions are determined in the model by grazing preferences for the food. These preferences are poorly constrained by observations (Buitenhuis et al., 2010), apart from the general observations that zooplankton tend to eat prey that are approximately 10 times smaller in equivalent spherical diameter (Straile, 1997). We therefore used observations of PFT distributions from the MAREDAT atlas (Buitenhuis, Vogt, et al., 2013, <http://ired.uea.ac.uk/web/green-ocean/data#biomass>) to select food preferences in the model (<http://opendap.uea.ac.uk:8080/opendap/hyrax/greenocean/PlankTOM12/contents.html>). We removed the biomass of *Gymnosomata*, which do not calcify, and those *Pseudosecosomata* which

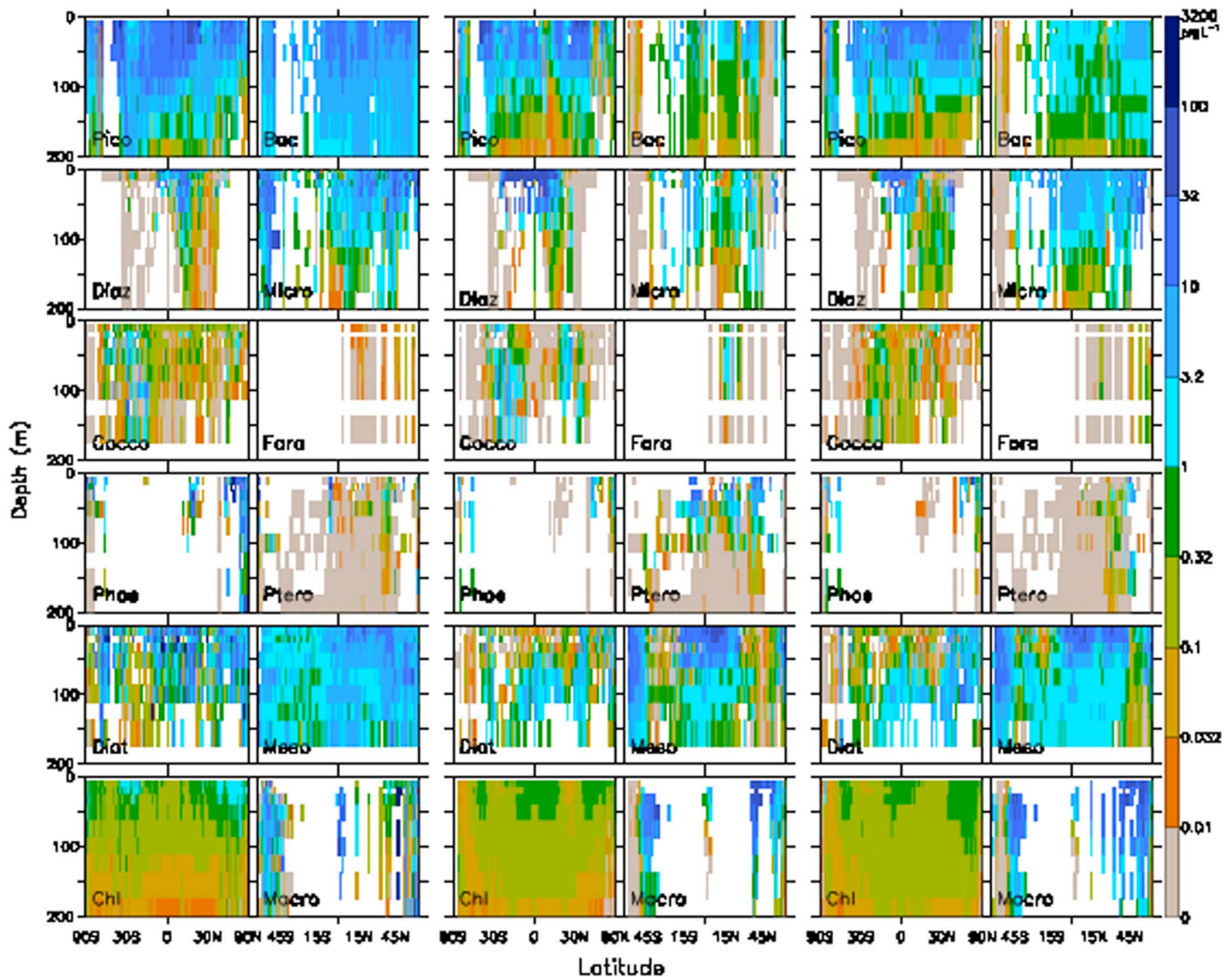


**Figure 4.** Zonal average biomass distribution of plankton functional types ( $\mu\text{g C/L}$ ) and total chlorophyll ( $\mu\text{g/L}$ ). Pico = picophytoplankton; Diaz =  $\text{N}_2$  fixers; Cocco = coccolithophores; Phae = *Phaeocystis sp.*; Diat = diatoms; Chl = chlorophyll *a*; Bac = *Bacteria + Archaea*; Micro = microzooplankton; Fora = foraminifers; Ptero = pteropods; Meso = mesozooplankton; Macro = macrozooplankton. Model results have been sampled where there are observations. (left two columns) MARine Ecosystem DATA observations, except chlorophyll from World Ocean Atlas 2005. (middle two columns) Standard model run. (right two columns) Model tuned to reproduce  $\text{CaCO}_3$  export without dissolution above the saturation horizons.

only calcify as larvae or as larvae and juveniles, from the MAREDAT database of total pteropod biomass. There is no biomass data on *Pseudosecosomata* which calcify during the whole life cycle, so all the data on pteropods that calcify during the whole life cycle are of *Euthecosomata* species. The biomass of pteropods that calcify during the whole life cycle was converted from ( $\text{CaCO}_3 + \text{POC}$ ) to POC using the  $\text{CaCO}_3:\text{POC}$  ratio given in section 3.1 (Buitenhuis et al., 2018). The total pteropod biomass database is described in Bednaršek et al. (2012), foraminifers in Schiebel and Movellan (2012), and coccolithophores in O'Brien et al. (2013).

### 3.3. Annual Cycle of Alkalinity

The amplitude of the annual alkalinity cycle was fit to  $\text{alkalinity}(t) = \text{amplitude} * \sin(t - \text{offset})$ . Amplitude and offset were optimized against the GLODAPv2 observations and the model results (which were subsampled where there were observations) using the golden-section approach described in Buitenhuis and Geider (2010). Only latitudes for which there were at least 5 months of observations were included.

**Table 1**  
Global  $\text{CaCO}_3$  Turnover Rates and Contributions by the Three Modeled PFTs

	Observations	Standard simulation	Exp simulation
$\text{CaCO}_3$ production	$1.1^a \rightarrow 1.6^b$ Pg C/year	4.7 Pg C/year	0.4 Pg C/year
Pteropods		89%	38%
Coccolithophores		8%	37%
Foraminifers		3%	25%
$\text{CaCO}_3$ export @ 100 m		0.6 Pg C/year	0.4 Pg C/year
Pteropods		33%	36%
$\text{CaCO}_3$ export @ 2,000 m	$0.4^c - 0.6^b \pm 0.4$ Pg C/year	0.5 Pg C/year	0.3 Pg C/year
Pteropods		12%	26%

<sup>a</sup>Lee (2001). <sup>b</sup>Berelson et al. (2007). <sup>c</sup>Honjo et al. (2008).

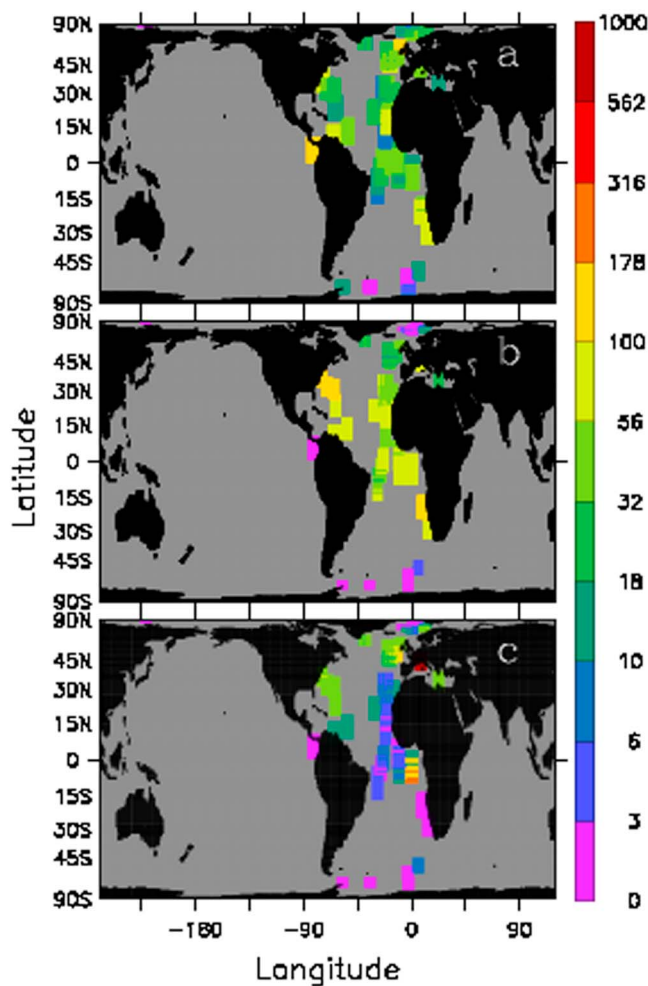


**Figure 5.** Depth-averaged sinking flux of  $\text{CaCO}_3$  ( $\text{mg}\cdot\text{m}^{-2}\cdot\text{day}^{-1}$ ). (a) Observations (Torres Valdés et al., 2014). (b) Standard model run. (c) Model tuned to reproduce  $\text{CaCO}_3$  export without dissolution above the saturation horizons.

## 4. Results

Analysis of the observations presented in section 3 shows that the average biomass of pteropods that calcify during the whole life cycle (Figures 2, 3a, and 4) constitutes 84% of the total biomass of pteropods (Bednaršek et al., 2012). The gridded database of the pteropods that calcify during the whole life cycle contains 6,850 data points, which is 99% of the data coverage of the total pteropod database. In the remainder of this paper where we refer to pteropods, we mean only pteropods that calcify during the whole life cycle. Above 50-m and below 250-m depth, the biomass of pteropods is up to an order of magnitude higher than that of foraminifers and coccolithophores (Figure 3a). In contrast, between 50 and 100 m, the biomass of pteropods is similar to that of coccolithophores, while between 125 and 250 m, it becomes lower than the biomass of coccolithophores but similar to that of foraminifers.

The observed growth rates of foraminifers are 2–6 times lower (Figures 1b and 1f) than that of pteropods, while the growth rates of coccolithophores are lower than that of pteropods in cold waters and higher in warm waters (Figures 1c and 1f).

Initial simulations with the model using parameterizations based directly on measured growth and respiration rates showed an underestimation of the biomass of all zooplankton PFTs. This underestimation could conceivably indicate that the available rate measurements are biased, for example, because experimental manipulation stresses the zooplankton. Because the underestimation is a general feature of the model, and there are quite a lot of data ( $n = 9,970$ ) to constrain these rates, the more likely explanation is that the underestimation is indicative of several survival strategies used by zooplankton that are not, or not sufficiently, included in the model, including switching between routine and basal respiration when food is scarce, and intra-PFT succession of species with slightly different ecological niches that maximize their success. In addition, some microzooplankton can enhance survival through mixotrophy and metazoan zooplankton through vertical migration. To correct for this bias, we decreased respiration rates for all zPFTs (e.g., Figures 1d and 1e) and adjusted food preferences to optimize the fit to biomass data. This is our “standard” model run presented here.

This standard model run produces a frequency distribution of biomass that is in the observed range (Figure 2). The model reproduces the observed vertical distributions of biomass within the uncertainty of the observations (Figure 3), and the observed latitudinal distributions for phytoplankton, and to a lesser extent for the picoheterotrophs and zooplankton (Figure 4). The  $\text{CaCO}_3$  production is 4.7 Pg C/year, with pteropods accounting for 89% of it (Table 1). Coccolithophores account for only 8% of  $\text{CaCO}_3$  production despite the fact that their growth rates are similar to those of pteropods (Figure 1f), because their  $\text{CaCO}_3/\text{POC}$  ratio is ~5 times lower (section 3.1). Foraminifers account for only 3% of  $\text{CaCO}_3$  because of their opposite characteristics of low growth rates and a  $\text{CaCO}_3/\text{POC}$  ratio that is similar to pteropods.

The model can only reproduce both the observed biomass distributions of the calcifiers and the average  $\text{CaCO}_3$  export by including substantial dissolution above the saturation horizon. In the standard model run, we attribute all the dissolution of  $\text{CaCO}_3$  above the saturation horizon to aragonite in order to calculate a conservative estimate of the contribution

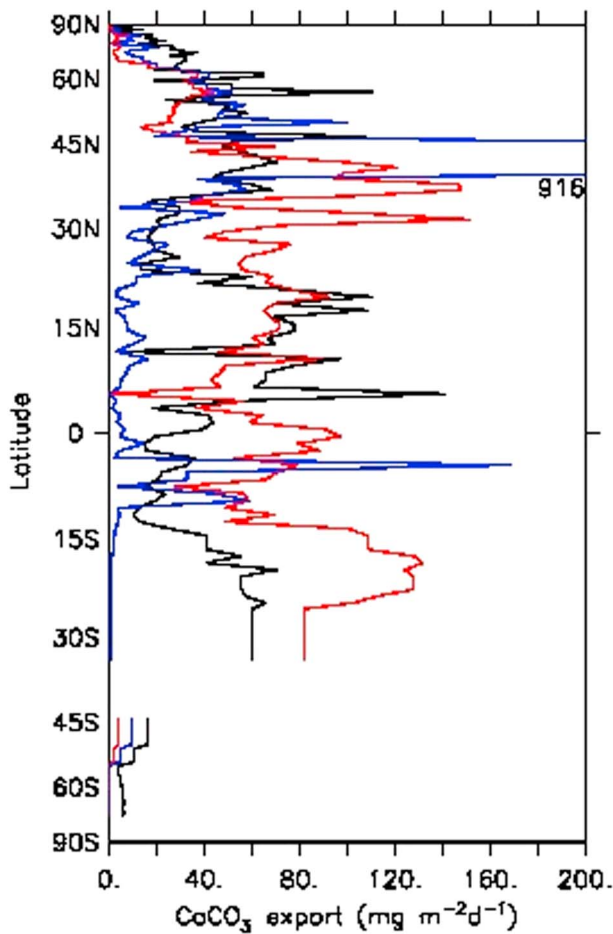


**Figure 6.**  $\text{CaCO}_3$  export ( $\text{mg}\cdot\text{m}^{-2}\cdot\text{day}^{-1}$ ) as a function of latitude (averaged over longitude, depth, and month). Model results have been sampled where there are observations. (black) Observations (Torres Valdés et al., 2014). (red) Standard model run. (blue) Model simulation optimized to reproduce  $\text{CaCO}_3$  export without dissolution above the saturation horizons. Very high  $\text{CaCO}_3$  export at shallow depth in the Mediterranean Sea in the latter model simulation are presumably due to repeated resuspension and settling of particulate matter near the sea bottom.

of pteropods to the global ocean  $\text{CaCO}_3$  export. *Conservative* here only refers to the contribution relative to coccolithophores and foraminifers. We note in the discussion that there are several other undercharacterized groups of calcifiers that could make the absolute estimates of the respective contributions smaller. The model reproduces the observed  $\text{CaCO}_3$  export observations (Figures 5–7) when 95% of aragonite is lost at the point where biogenic  $\text{CaCO}_3$  gets converted to detrital  $\text{CaCO}_3$ . In the standard simulation the contribution of pteropods to  $\text{CaCO}_3$  export is 33% of the total 0.6 Pg C/year at 100-m depth, decreasing to 12% at 2,000 m (Table 1) and only 1% at 4,000 m, reflecting the higher solubility of aragonite. The model has only one pool of sinking calcite, to which both coccolithophores and foraminifers contribute, but their contributions to calcite export would be roughly proportional to their contributions to calcite production.

In the alternative “exp” simulation, we tune the model to reproduce the observed  $\text{CaCO}_3$  export without relying on dissolution above the saturation horizons. As with the standard simulation, we changed the exp simulation aiming to decrease only pteropod biomass. We do this in order to get a conservative estimate of the contribution of pteropods to global  $\text{CaCO}_3$ , even though the database of foraminifers has the fewest data points with the smallest geographical spread (Buitenhuis, Vogt, et al., 2013), so from the perspective of data constraints, we should have decreased the foraminifer biomass. In the exp simulation, the spatial variability of the calcifier biomass distributions has decreased dramatically (Figure 2), while the variability of  $\text{CaCO}_3$  export has increased (Figure 5). Turnover times of calcifier biomass and associated  $\text{CaCO}_3$  are relatively constant between the simulations (5–7 days for pteropods, 5–6 days for coccolithophores, and 25–35 days for foraminifers), so there is possibly a switch from a dominance of bottom-up control of production rates to top-down control of biomass. While interesting from a macroecological point of view, it fell outside the scope of this study to resolve how quite modest changes in parameters caused this switch. In the exp simulation, pteropods again dominate the  $\text{CaCO}_3$  production with 38% of the total 0.4 Pg C/year, even though they contribute only 13% to the total calcifier biomass. Coccolithophores produce almost as much as 37%, and foraminifers produce 25%. The contribution of pteropods to  $\text{CaCO}_3$  export is 36% at 100 m.

Since the standard model run shows much higher gross  $\text{CaCO}_3$  production than has previously been suggested (Table 1), we evaluate our results against two additional observational databases. First, we compiled a small database to evaluate aragonite production and export in the two model runs. As always with comparisons of model results to measurements in the ocean (e.g., Buitenhuis et al., 2006), point-by-point comparisons are quite poor (Figure 8). Nevertheless, from the database as a whole, it is clear that the exp model run with no dissolution above the saturation horizons consistently underestimates the observations.

Second, we compared the seasonal cycle of alkalinity in the GLODAPv2 observations (Olsen et al., 2016) to the standard model run (Figure 9). If  $\text{CaCO}_3$  production had been overestimated, we would expect the seasonal cycle of alkalinity to have too large an amplitude compared to the observations. This is generally not the case ( $\text{amplitude}_{\text{model}} = 0.6 \cdot \text{amplitude}_{\text{observations}} + 10$ ,  $p < 0.001$ , Figure 9c), although the amplitude is larger than the observations between 46° and 62°N.

## 5. Discussion

We show that model results can be reconciled with both observations of biomass of the three main types of marine planktic calcifiers (pteropods, coccolithophores, and foraminifers, Figure 2) and with observations of

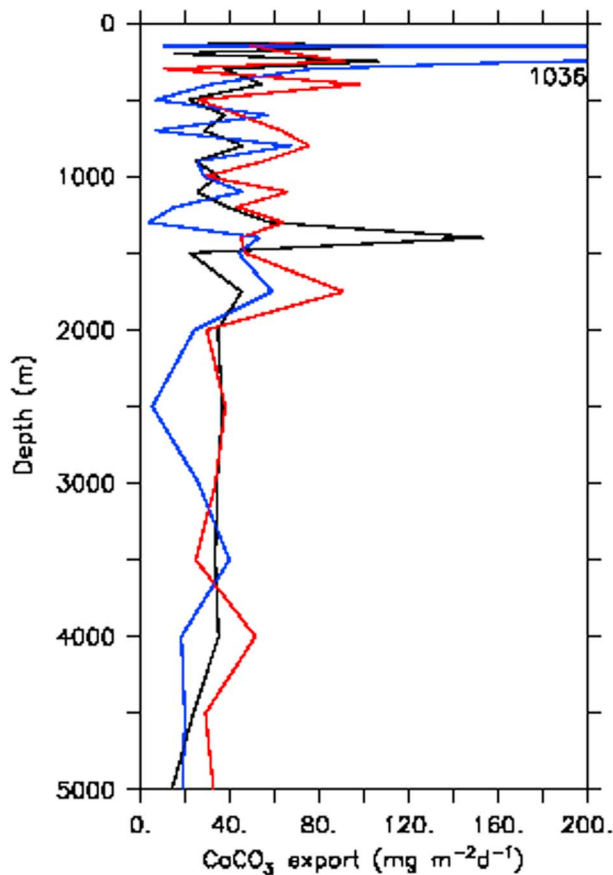


**Figure 7.**  $\text{CaCO}_3$  export ( $\text{mg}\cdot\text{m}^{-2}\cdot\text{day}^{-1}$ ) as a function of depth. Model results have been sampled where there are observations. (black) Observations (Torres Valdés et al., 2014). (red) Standard model run. (blue) Model simulation optimized to reproduce  $\text{CaCO}_3$  export without dissolution above the saturation horizons. Very high  $\text{CaCO}_3$  export at shallow depth in the Mediterranean Sea in the latter model simulation are presumably due to repeated resuspension and settling of particulate matter near the sea bottom.

$\text{CaCO}_3$  export (Figures 6 and 7) but only when introducing substantial dissolution of  $\text{CaCO}_3$  above the saturation horizon. Betzer et al. (1984) also showed a substantial decrease in pteropod fluxes above the saturation horizon between 100- and 400-m depths. Our results suggest that pteropods play a substantial role for the cycle of  $\text{CaCO}_3$  in the ocean, contributing up to 89% of the pelagic calcification and at least 33% of the export at 100 m.

There is one major caveat to this apparent dissolution. Collier et al. (2000) present observations that suggest the pteropods in sediment traps are not swimmers, so the common, though by no means universal, procedure of removing all pteropods, dead or alive, from sediment trap samples (as recommended by, e.g., Buesseler et al., 2007) could have led to underestimation of  $\text{CaCO}_3$  export, which would be an alternate explanation that could reconcile the high calcifier biomass and turnover rates with the observed  $\text{CaCO}_3$  flux in sediment traps. In addition to the very small observational record used by Milliman (1993), this could have misled him into concluding that pteropods contribute little to  $\text{CaCO}_3$  export, which has become a mostly implicit, accepted view in carbonate budgets since then. Measurement and reporting of the “swimmer” biomass in flux units would allow analysis of whether this potential flux is large enough to close the budget without dissolution above the saturation horizon. However, this caveat does not offer an alternative explanation for why the data in Figures 2 and 8 fit much better with substantial dissolution above the saturation horizon than without, so based on currently available data, the high production-high dissolution standard model run is still the only way to reproduce all observations. The unjustified removal of pteropods from sediment trap samples could be a smaller contributor to help close the gap between high calcifier biomasses and low deep ocean  $\text{CaCO}_3$  flux. Our analysis provides supporting evidence for  $\text{CaCO}_3$  dissolution above the saturation horizon, independent of the previously used TA\* method (Feely et al., 2004), which Friis et al. (2006) showed to be inconclusive.

Although  $\text{CaCO}_3$  dissolution in supersaturated surface waters of 25%/day has been observed in a bloom of the calcite producing coccolithophore *Emiliania huxleyi* (Buitenhuis et al., 1996), in the standard simulation, we have attributed all  $\text{CaCO}_3$  dissolution to the more soluble aragonite,

in order to arrive at a conservative estimate of the contribution of pteropods/aragonite. More such dissolution experiments would help in decreasing the uncertainties associated with the  $\text{CaCO}_3$  budget (Figure 8).

Likewise, in the exp simulation, we have attempted to only decrease the pteropod biomass, even though the database of foraminifers is smallest. During model tuning, the foraminifera biomass was very sensitive to changes in parameters, including the parameters of the other PFTs, suggesting that the ecological niche of foraminifers is the least well defined by the available data. Possibly as a consequence, the contribution of foraminifera to  $\text{CaCO}_3$  export had the largest relative variation between the two simulations, from 18–26%, while the contribution of pteropods showed the least variation, from 33–36%.

When we compare the seasonal cycles of alkalinity in the observations and in the standard model run, the amplitudes in the model are actually underestimated (Figure 9), even though the gross  $\text{CaCO}_3$  production is 4.7 Pg C/year, while Lee (2001) calculates a  $\text{CaCO}_3$  production of 1.1 Pg C/year based on the seasonal cycle of alkalinity (we also use an updated database of alkalinity). We conclude that what the method of Lee (2001) detects is much closer to net than to gross annual  $\text{CaCO}_3$  production. This makes sense in terms of the short turnover times of living biomass and attached  $\text{CaCO}_3$  (5–35 days). While the transient nature of the gross production that dissolves in the upper ocean means it does not

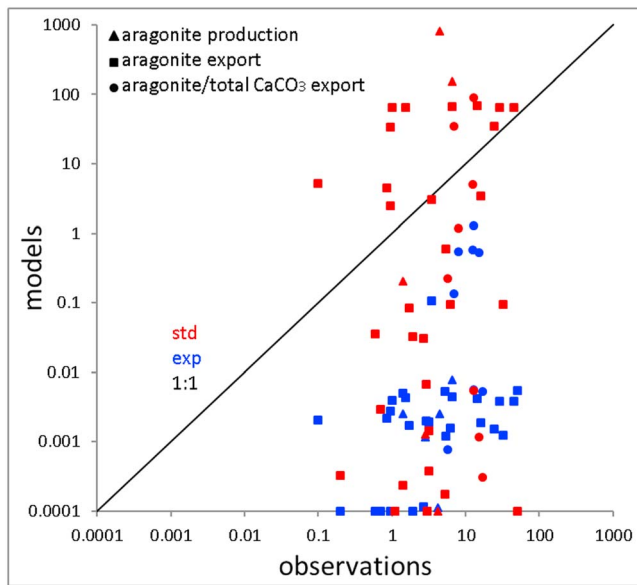


**Figure 8.** Aragonite production (triangles,  $\text{mg}\cdot\text{m}^{-2}\cdot\text{day}^{-1}$ ), aragonite export (squares,  $\text{mg}\cdot\text{m}^{-2}\cdot\text{day}^{-1}$ ) and aragonite export/total  $\text{CaCO}_3$  export (circles, %; Bednaršek et al., 2012; Berner & Honjo, 1981; Betzer et al., 1984; Fabry, 1989, 1990; Fabry & Deuser, 1991); x axis: observations, y axis model results at the same place and month. (red) Standard model run. (blue) Model simulation optimized to reproduce  $\text{CaCO}_3$  export without dissolution above the saturation horizons. Model values  $\leq 0.0001$  are shown as 0.0001.

affect the  $\text{CaCO}_3$  budget; including it allows us to use all available observations to constrain the model. The estimate of Berelson et al. (2007) is based on an evaluation of different published methods, and they acknowledge that their estimate of 1.6 Pg C/year is a minimum value (Table 1).

We have estimated the contribution of the three calcifying groups that have been suggested to be major contributors to the global ocean  $\text{CaCO}_3$  budget in this paper. There are at least five more groups of pelagic marine calcifiers whose contribution is thought to be smaller: fish, heteropods, calcifying ostracods, dinoflagellates, and ciliates. However, in view of our reassessment of the contribution of pteropods, it seems warranted to more accurately assess the importance of these other groups and obtain a full picture of the production and loss terms for  $\text{CaCO}_3$ . Wilson et al. (2009) estimated the contribution of fish to  $\text{CaCO}_3$  production to be 3–15%, based on an extrapolation of measurements on relatively large fish to the higher turnover rates of organic carbon in small fish. Schiebel (2002) estimated the contribution of calcifying dinoflagellates to  $\text{CaCO}_3$  export to be 3.5%, based on a surface sediment dataset that is limited to the low-latitude Atlantic Ocean. Even less information is available on the physiology and biomass distribution of these groups than on the three groups we have modeled here, and therefore, both the work of gathering the data and synthesizing it are yet to be done.

In conclusion, we show both bottom-up (Figures 1 and 2) and top-down (Figure 8) evidence for a substantial contribution of pteropods to the global  $\text{CaCO}_3$  budget, for example, a contribution to  $\text{CaCO}_3$  export of about 35%, characterized by high production rates and high dissolution rates. The simulation that is consistent with all the evidence that we bring to bear on this question shows much higher  $\text{CaCO}_3$  production (4.7 Pg C/year) than previous studies but is still consistent with the seasonal cycle of upper ocean alkalinity (Figure 9) and  $\text{CaCO}_3$  export at 2,000-m depth of 0.6 Pg C/year (Figure 7). Because aragonite is more soluble than the calcite that, as far as we are aware, is used exclusively by all other global ocean biogeochemical models, the sensitivity of the alkalinity cycle to ocean acidification and the associated capacity of the ocean to take up future anthropogenic  $\text{CO}_2$  emission needs to be reexamined.

Figure 9 consists of three panels: (a) a heatmap of observed alkalinity anomalies, (b) a heatmap of standard model run alkalinity anomalies, and (c) a line plot of the amplitude of the seasonal cycle. Panel (a) shows observed alkalinity anomalies averaged over the top 50 m ( $\mu\text{eq/L}$ ) versus month and latitude. Panel (b) shows the standard model run sampled where there are observations. Panel (c) shows the amplitude of the seasonal cycle, with black lines for observations and red lines for the standard model run. The color scale for panels (a) and (b) ranges from -200 to 200  $\mu\text{eq/L}$ .

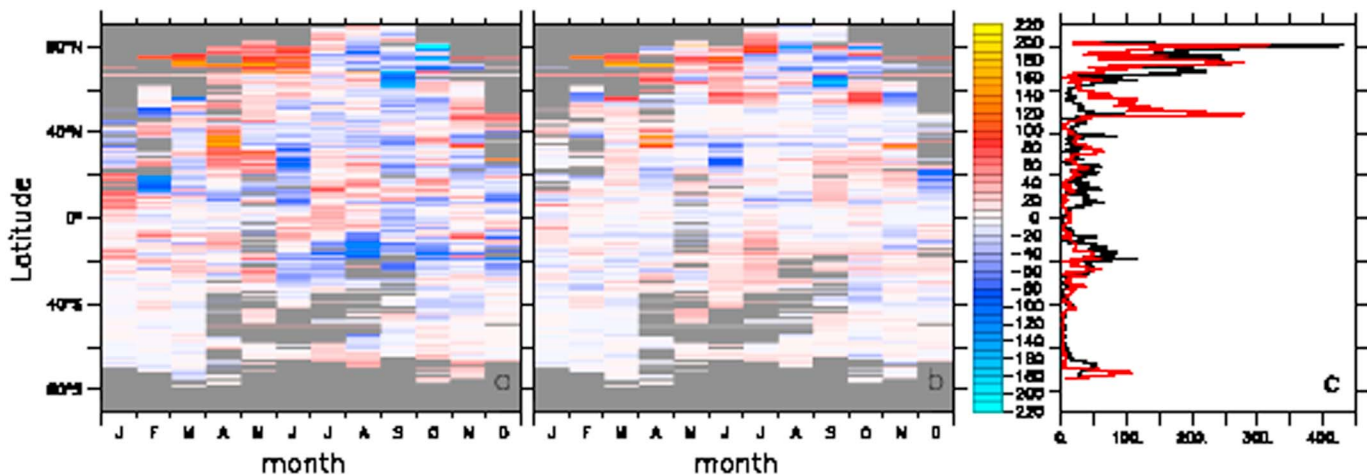


**Figure 9.** Alkalinity anomaly averaged over the top 50 m ( $\mu\text{eq/L}$ ) versus month and latitude. (a) GLODAPv2 (Olsen et al., 2016). (b) Standard model run sampled where there are observations. (c) Amplitude of the seasonal cycle. (black) Observations. (red) Standard model run.

## Acknowledgments

This research was funded by the European Union through the EMBRACE project (FP7 grant 282672). The observational data are available at <https://ired.uea.ac.uk/web/green-ocean/data#biomass>. Output of the standard model simulation is available at <http://opendap.uea.ac.uk:8080/opendap/hyrax/greenocean/PlankTOM12/>. We thank Nina Keul and an anonymous reviewer for their helpful comments.

## References

- Bednaršek, N., Harvey, C. J., Kaplan, I. C., Feely, R. A., & Možina, J. (2016). Pteropods on the edge: Cumulative effects of ocean acidification, warming, and deoxygenation. *Progress in Oceanography*, *145*, 1–24. <https://doi.org/10.1016/j.pocean.2016.04.002>
- Bednaršek, N., Možina, J., Vogt, M., O'Brien, C., & Tarling, G. A. (2012). The global distribution of pteropods and their contribution to carbonate and carbon biomass in the modern ocean. *Earth System Science Data*, *5*(2), 227–239. <https://doi.org/10.5194/essd-5-227-2013>
- Berelson, W. M., Balch, W. M., Najjar, R., Feely, R. A., Sabine, C., & Lee, K. (2007). Relating estimates of  $\text{CaCO}_3$  production, export, and dissolution in the water column to measurements of  $\text{CaCO}_3$  rain ratio into sediment traps and dissolution on the sea floor: A revised global carbonate budget. *Global Biogeochemical Cycles*, *21*, GB1024. <https://doi.org/10.1029/2006GB002803>
- Berner, R. A., & Honjo, S. (1981). Pelagic sedimentation of aragonite: Its geochemical significance. *Science*, *211*(4485), 940–942. <https://doi.org/10.1126/science.211.4485.940>
- Betzer, P. R., Byrne, R. H., Acker, J. G., Lewis, C. S., Jolley, R. R., & Feely, R. A. (1984). The oceanic carbonate system—A reassessment of biogenic control. *Science*, *226*(4678), 1074–1077. <https://doi.org/10.1126/science.226.4678.1074>
- Buesseler, K. O., Antia, A. N., Chen, M., Fowler, S. W., Gardner, W. D., Gustafsson, O., et al. (2007). An assessment of the use of sediment traps for estimating upper ocean particle fluxes. *Journal of Marine Research*, *65*, 345–416.
- Buitenhuis, E., Hashioka, T., & Le Quéré, C. (2013). Combined constraints on global ocean primary production using observations and models. *Global Biogeochemical Cycles*, *27*, 847–858. <https://doi.org/10.1002/gbc.20074>
- Buitenhuis, E. T., & Geider, R. J. (2010). A model of phytoplankton acclimation to iron-light colimitation. *Limnology and Oceanography*, *55*, 714–724. <https://doi.org/10.4319/lo.2010.55.2.0714>
- Buitenhuis, E., Rivkin, R., Salliey, S., & Le Quéré, C. (2010). Biogeochemical fluxes through microzooplankton. *Global Biogeochemical Cycles*, *24*, GB4015. <https://doi.org/10.1029/2009GB003601>
- Buitenhuis, E., van Bleijswijk, J., Bakker, D., & Veldhuis, M. (1996). Trends in inorganic and organic carbon in a bloom of *Emiliania huxleyi* in the North Sea. *Marine Ecology Progress Series*, *143*, 271–282. <https://doi.org/10.3354/meps143271>
- Buitenhuis, E., van der Wal, P., & de Baar, H. (2001). Blooms of *Emiliania huxleyi* are sinks of atmospheric carbon dioxide; A field and mesocosm study derived simulation. *Global Biogeochemical Cycles*, *15*(3), 577–587. <https://doi.org/10.1029/2000GB001292>
- Buitenhuis, E. T., Le Quéré, C., Aumont, O., Beaugrand, G., Bunker, A., Hirst, A., et al. (2006). Biogeochemical fluxes through mesozooplankton. *Global Biogeochemical Cycles*, *20*, GB2003. <https://doi.org/10.1029/2005GB002511>
- Buitenhuis, E. T., Le Quéré, C., Bednaršek, N., & Schiebel, R. (2018). Global database of Euthecosomata (calcified pteropods) biomass. *PANGAEA*. <https://doi.org/10.1594/PANGAEA.893745>
- Buitenhuis, E. T., Vogt, M., Moriarty, R., Bednaršek, N., Doney, S., Leblanc, K., et al. (2013). MAREDAT: Towards a World Ocean Atlas of marine ecosystem data. *Earth System Science Data*, *5*(2), 227–239. <https://doi.org/10.5194/essd-5-227-2013>
- Byrne, R. H., Acker, J. G., Betzer, P. R., Feely, R. A., & Cates, M. H. (1984). Water column dissolution of aragonite in the Pacific Ocean. *Nature*, *312*(5992), 321–326. <https://doi.org/10.1038/312321a0>
- Collier, R., Dymond, J., Honjo, S., Manganini, S., Francois, R., & Dunbar, R. (2000). The vertical flux of biogenic and lithogenic material in the Ross Sea: Moored sediment trap observations 1996–1998. *Deep-Sea Research Part II*, *47*(15–16), 3491–3520. [https://doi.org/10.1016/S0967-0645\(00\)00076-X](https://doi.org/10.1016/S0967-0645(00)00076-X)
- Enright, C., & Buitenhuis, E. T. (2014). Description of the PlankTOM10 equations. Retrieved from <http://www.biogeosciences-discuss.net/12/11935/2015/bgd-12-11935-2015-supplement.zip>
- Fabry, V. J. (1989). Aragonite production by pteropod molluscs in the subarctic Pacific. *Deep Sea Research*, *36*(11), 1735–1751. [https://doi.org/10.1016/0198-0149\(89\)90069-1](https://doi.org/10.1016/0198-0149(89)90069-1)
- Fabry, V. J. (1990). Shell growth rates of pteropod and heteropod molluscs and aragonite production in the open ocean: Implications for the marine carbonate system. *Journal of Marine Research*, *48*(1), 209–222. <https://doi.org/10.1357/002224090784984614>
- Fabry, V. J., & Deuser, W. G. (1991). Aragonite and magnesian calcite fluxes to the deep Sargasso Sea. *Deep Sea Research*, *38*(6), 713–728. [https://doi.org/10.1016/0198-0149\(91\)90008-4](https://doi.org/10.1016/0198-0149(91)90008-4)
- Feely, R. A., Sabine, C. L., Lee, K., Berelson, W., Kleypass, J., Fabry, V. J., & Millero, F. J. (2004). Impact of anthropogenic  $\text{CO}_2$  on the  $\text{CaCO}_3$  system in the oceans. *Science*, *305*(5682), 362–366. <https://doi.org/10.1126/science.1097329>
- Friis, K., Najjar, R. G., Follows, M. J., & Dutkiewicz, S. (2006). Possible overestimation of shallow-depth calcium carbonate dissolution in the ocean. *Global Biogeochemical Cycles*, *20*, GB4019. <https://doi.org/10.1029/2006GB002727>
- Gangstø, R., Gehlen, M., Schneider, B., Bopp, L., Aumont, O., & Joos, F. (2008). Modeling the marine aragonite cycle: Changes under rising carbon dioxide and its role in shallow water  $\text{CaCO}_3$  dissolution. *Biogeosciences*, *5*(4), 1057–1072. <https://doi.org/10.5194/bg-5-1057-2008>
- Gehlen, M., Gangstø, R., Schneider, B., Bopp, L., Aumont, O., & Ethe, C. (2007). The fate of pelagic  $\text{CaCO}_3$  production in a high  $\text{CO}_2$  ocean: A model study. *Biogeosciences*, *4*(4), 505–519. <https://doi.org/10.5194/bg-4-505-2007>
- Heinle, M. (2013). The effects of light, temperature and nutrients on coccolithophores and implications for biogeochemical models. (PhD thesis). Retrieved from [https://ueaeprints.uea.ac.uk/48676/1/thesis\\_Heinle.pdf](https://ueaeprints.uea.ac.uk/48676/1/thesis_Heinle.pdf)
- Honjo, S., Manganini, S. J., Krishfield, R. A., & Francois, R. (2008). Particulate organic carbon fluxes to the ocean interior and factors controlling the biological pump: A synthesis of global sediment trap programs since 1983. *Progress in Oceanography*, *76*(3), 217–285. <https://doi.org/10.1016/j.pocean.2007.11.003>
- Le Quéré, C., Buitenhuis, E. T., Moriarty, R., Alvain, S., Aumont, O., Bopp, L., et al. (2016). Role of zooplankton dynamics for Southern Ocean phytoplankton biomass and global biogeochemical cycles. *Biogeosciences*, *13*(14), 4111–4133. <https://doi.org/10.5194/bg-13-4111-2016>
- Le Quéré, C., Harrison, S. P., Prentice, I. C., Buitenhuis, E. T., Aumont, O., Bopp, L., et al. (2005). Ecosystem dynamics based on plankton functional types for global ocean biogeochemistry models. *Global Change Biology*. <https://doi.org/10.1111/j.1365-2486.2005.1004.x>
- Lee, K. (2001). Global net community production estimated from the annual cycle of surface water total dissolved inorganic carbon. *Limnology and Oceanography*, *46*(6), 1287–1297. <https://doi.org/10.4319/lo.2001.46.6.1287>
- Lombard, F., Labeyrie, L., Michel, E., Spero, H. J., & Lea, D. W. (2009). Modelling the temperature dependent growth rates of planktic foraminifera. *Marine Micropaleontology*, *70*, 1–7. <https://doi.org/10.1016/j.marmicro.2008.09.004>
- Lombard, F., Labeyrie, L., Michel, E., Bopp, L., Cortijo, E., Retailleau, S., et al. (2011). Modelling planktic foraminifer growth and distribution using an ecophysiological multi-species approach. *Biogeosciences*, *8*, 853–873. <https://doi.org/10.5194/bg-8-853-2011>
- Madec, G. (2008). NEMO ocean engine. Note du Pole de modelisation, Institut Pierre-Simon Laplace (IPSL), France, No 27. Retrieved from [http://www.nemo-ocean.eu/content/download/21612/97924/file/NEMO\\_book\\_3\\_4.pdf](http://www.nemo-ocean.eu/content/download/21612/97924/file/NEMO_book_3_4.pdf)
- Milliman, J. D. (1993). Production and accumulation of calcium carbonate in the ocean: budget of a nonsteady state. *Global Biogeochemical Cycles*, *7*, 927–957.

- Milliman, J. D., Troy, P. J., Balch, W. M., Adams, A. K., Li, Y.-H., & Mackenzie, F. T. (1999). Biologically mediated dissolution of calcium carbonate above the chemical lysocline? *Deep Sea Research, Part I*, *46*, 1653–1669.
- Moriarty, R. (2009). Role of macro-zooplankton for the global carbon cycle. (PhD thesis). Retrieved from [https://ueaeprints.uea.ac.uk/10605/1/Thesis\\_moriarty\\_r\\_2009.pdf](https://ueaeprints.uea.ac.uk/10605/1/Thesis_moriarty_r_2009.pdf)
- O'Brien, C. J., Peloquin, J. A., Vogt, M., Heinle, M., Gruber, N., Ajani, P., et al. (2013). Global marine plankton functional type biomass distributions: Coccolithophores. *Earth System Science Data*, *5*(2), 259–276. <https://doi.org/10.5194/essd-5-259-2013>
- Olsen, A., Key, R. M., van Heuven, S., Lauvset, S. K., Velo, A., Lin, X., et al. (2016). The Global Ocean Data Analysis Project version 2 (GLODAPv2)—An internally consistent data product for the world ocean. *Earth System Science Data*, *8*(2), 297–323. <https://doi.org/10.5194/essd-8-297-2016>
- Schiebel, R. (2002). Planktic foraminiferal sedimentation and the marine calcite budget. *Global Biogeochemical Cycles*, *16*(4), 1065. <https://doi.org/10.1029/2001GB001459>
- Schiebel, R., Barker, S., Lendt, R., Thomas, H., & Bollmann, J. (2007). Planktic foraminiferal dissolution in the twilight zone. *Deep-Sea Research Part II*, *54*(5-7), 676–686. <https://doi.org/10.1016/j.dsr2.2007.01.009>
- Schiebel, R., & Movellan, A. (2012). First-order estimate of the planktic foraminifer biomass in the modern ocean. *Earth System Science Data*, *4*(1), 75–89. <https://doi.org/10.5194/essd-4-75-2012>
- Straille, D. (1997). Gross growth efficiencies of protozoan and metazoan zooplankton and their dependence on food concentration, predator-prey weight ratio, and taxonomic group. *Limnology and Oceanography*, *42*(6), 1375–1385.
- Torres Valdés, S., Painter, S. C., Martin, A. P., Sanders, R., & Felden, J. (2014). Data compilation of fluxes of sedimenting material from sediment traps in the Atlantic Ocean. *Earth System Science Data*, *6*(1), 123–145. <https://doi.org/10.5194/essd-6-123-2014>
- Wilson, R. W., Millero, F. J., Taylor, J. R., Walsh, P. J., Christensen, C., Jennings, S., & Grosell, M. (2009). Contribution of fish to the marine inorganic carbon cycle. *Science*, *323*(5912), 359–362. <https://doi.org/10.1126/science.1157972>